

Video Article

Fabrication of a Bioactive, PCL-based "Self-fitting" Shape Memory Polymer Scaffold

Lindsay N. Nail¹, Dawei Zhang^{2,3}, Jessica L. Reinhard¹, Melissa A. Grunlan^{1,2}

¹Department of Biomedical Engineering, Texas A&M University

²Department of Material Science and Engineering, Texas A&M University

³Institute of Advanced Materials and Technology, University of Science & Technology Beijing

Correspondence to: Melissa A. Grunlan at mgrunlan@tamu.edu

URL: <https://www.jove.com/video/52981>

DOI: [doi:10.3791/52981](https://doi.org/10.3791/52981)

Keywords: Bioengineering, Issue 104, Shape memory, polycaprolactone, polydopamine, scaffold, salt template, bioactive, bone healing

Date Published: 10/23/2015

Citation: Nail, L.N., Zhang, D., Reinhard, J.L., Grunlan, M.A. Fabrication of a Bioactive, PCL-based "Self-fitting" Shape Memory Polymer Scaffold. *J. Vis. Exp.* (104), e52981, doi:10.3791/52981 (2015).

Abstract

Tissue engineering has been explored as an alternative strategy for the treatment of critical-sized cranio-maxillofacial (CMF) bone defects. Essential to the success of this approach is a scaffold that is able to conformally fit within an irregular defect while also having the requisite biodegradability, pore interconnectivity and bioactivity. By nature of their shape recovery and fixity properties, shape memory polymer (SMP) scaffolds could achieve defect "self-fitting." In this way, following exposure to warm saline (~60 °C), the SMP scaffold would become malleable, permitting it to be hand-pressed into an irregular defect. Subsequent cooling (~37 °C) would return the scaffold to its relatively rigid state within the defect. To meet these requirements, this protocol describes the preparation of SMP scaffolds prepared via the photochemical cure of biodegradable polycaprolactone diacrylate (PCL-DA) using a solvent-casting particulate-leaching (SCPL) method. A fused salt template is utilized to achieve pore interconnectivity. To realize bioactivity, a polydopamine coating is applied to the surface of the scaffold pore walls. Characterization of self-fitting and shape memory behaviors, pore interconnectivity and *in vitro* bioactivity are also described.

Video Link

The video component of this article can be found at <https://www.jove.com/video/52981/>

Introduction

Currently considered the gold standard of cranio-maxillofacial (CMF) bone defect treatments, transplantation of harvested autologous grafts is hindered by complex grafting procedures, donor site morbidity and limited availability¹. A particular difficulty is shaping and fixing the rigid autograft tightly into the defect in order to obtain osseointegration and to prevent graft resorption. Tissue engineering has been investigated as an alternative strategy to autografting and synthetic bone substitutes (e.g. bone cement)^{2,3}. Critical to the success of a tissue engineering approach is a scaffold with a specific set of properties. First, in order to achieve osseointegration, the scaffold must form close contact with adjacent bone tissue⁴. The scaffold should also be osteoconductive, permitting cell migration, nutrient diffusion and neotissue deposition^{4,5}. This behavior is generally achieved with biodegradable scaffolds exhibiting a highly interconnected pore morphology. Lastly, the scaffold should be bioactive so as to promote integration and bonding with surrounding bone tissue⁵.

Here, we present a protocol to prepare a tissue engineering scaffold with these properties. Importantly, this scaffold exhibits the ability to "self-fit" into irregular CMF defects due to its shape memory behavior⁶. Thermoresponsive shape memory polymers (SMPs) are known to undergo shape change upon exposure to heat^{7,8}. SMPs are comprised of "netpoints" (i.e. chemical or physical crosslinks) which determine the permanent shape and "switching segments" which maintain the temporary shape and recover the permanent shape. The switching segments exhibit a thermal transition temperature (T_{trans}) corresponding to either the glass transition (T_g) or melt transition (T_m) of the polymer. As a result, SMPs may be sequentially deformed into a temporary shape at $T > T_{trans}$, fixed in the temporary shape at $T < T_{trans}$, and recovered to the permanent shape at $T > T_{trans}$. Thus, an SMP scaffold could achieve "self-fitting" within a CMF defect as follows⁶. After exposure to warm saline ($T > T_{trans}$), an SMP scaffold would become malleable, permitting a generically prepared cylindrical scaffold to be hand-pressed into an irregular defect, with shape recovery promoting expansion of the scaffold to the defect boundary. Upon cooling ($T < T_{trans}$), the scaffold would return to its relatively more rigid state, with shape fixity maintaining its new temporary shape within the defect. In this protocol, an SMP scaffold is prepared from polycaprolactone (PCL), a biodegradable polymer studied extensively for tissue regeneration and other biomedical applications⁹⁻¹¹. For shape memory, the T_m of PCL serves as the T_{trans} and varies between 43 and 60 °C, depending on the molecular weight of the PCL¹². In this protocol, the T_{trans} (i.e. T_m) of the scaffold is 56.6±0.3 °C⁶.

In order to achieve osteoconductivity, a protocol was developed to make PCL-based SMP scaffolds with highly interconnected pores based on a solvent-casting particulate-leaching (SCPL) method^{6,13,14}. Polycaprolactone diacrylate (PCL-DA) (M_n = ~10,000 g/mol) was utilized to permit rapid, photochemical crosslinking and was dissolved in dichloromethane (DCM) to allow solvent-casting over the salt template. Following

photochemical cure and solvent evaporation, the salt template was removed by leaching into water. The average salt size regulates scaffold pore size. Importantly, the salt template was fused with water prior to solvent-casting to achieve pore interconnectivity.

Bioactivity was imparted to the SMP scaffold by the *in situ* formation of a polydopamine coating onto pore walls⁶. Bioactivity is often introduced into scaffolds by the inclusion of glass or glass-ceramic fillers¹⁵. However, these may give rise to unwanted brittle mechanical properties. Dopamine has been shown to form an adherent, thin polydopamine layer on a variety of substrates¹⁶⁻¹⁹. In this protocol, the SMP scaffold was subjected to a slightly basic solution (pH = 8.5) of dopamine to form a nanothick coating of polydopamine on all pore wall surfaces⁶. In addition to enhancing surface hydrophilicity for improved cell adhesion and spreading, polydopamine has been shown to be bioactive in terms of formation of hydroxyapatite (HAp) upon exposure to simulated body fluid (SBF)^{18,20,21}. In a last step, the coated scaffold is exposed to heat treatment at 85 °C ($T > T_{trans}$) which leads to scaffold densification. Heat treatment was previously noted to be essential for scaffold shape memory behavior, perhaps due to PCL crystalline domains reorganizing to closer proximity¹⁴.

We additionally describe the methods to characterize the self-fitting behavior within an irregular model defect, shape memory behavior in terms strain-controlled cyclic-thermal mechanical compression tests (*i.e.* shape recovery and shape fixity), pore morphology, and *in vitro* bioactivity. Strategies to tailor scaffold properties are also presented.

Protocol

1. Synthesizing PCL-DA Macromer

- Run the acrylation reaction.
 - Weigh 20 g of PCL-diol ($M_n = \sim 10,000$ g/mol) into a 250 ml round bottom flask equipped with a Teflon-covered magnetic stir bar.
 - Dissolve the PCL-diol in DCM.
 - Add 120 mL of DCM to the flask (concentration = 0.17 g/ml).
 - Place a rubber septum loosely into the neck of the flask so as to avoid pressure build-up while also preventing evaporation of DCM.
 - Stir solution for ~30 min at ~250 rpm to completely dissolve the polymer.
 - Add ~6.6 mg of 4-dimethylaminopyridine (DMAP) to the solution and dissolve with stirring.
 - Place a rubber septum securely into the neck of the flask. Allow the solution to continue stirring.
 - Through the rubber septum, gently purge the flask with N_2 for ~3 min by using a positive N_2 pressure needle inlet and an open needle as an outlet.
 - Remove the N_2 inlet and outlet.
 - Add 0.56 ml (4.0 mmol) of triethylamine (Et_3N) dropwise via a glass syringe equipped with a needle inserted through the rubber septum.
 - Add 0.65 ml (8.0 mmol) of acryloyl chloride dropwise via a glass syringe equipped with a needle inserted through the rubber septum.
 - Return the N_2 inlet to the flask and allow the contents to stir under positive N_2 pressure for ~30 min.
 - Pre-heat an oil bath to 55 °C.
 - After the allotted ~30 min, remove the N_2 inlet and replace the septum with a condenser.
 - Submerge the flask into the pre-heated oil bath.
 - Allow the contents of the flask to stir for 20 hr.
 - After the allotted 20 hr, remove the flask from the oil bath and allow contents to cool to RT.
 - Using a rotary evaporator, remove DCM solvent from the flask.
- Purify the crude PCL-DA product.
 - To the flask, add ~135 ml of ethyl acetate and dissolve the crude PCL-DA.
 - Gravity filter the solution through filter paper into a clean 250 ml round bottom flask. (Note: Solution may thicken on the filter paper, not readily passing through. If so, carefully apply mild heat with a heating gun.)
 - Using a rotary evaporator, remove ethyl acetate solvent from the flask.
 - To the flask, add ~140 ml of DCM and dissolve the crude PCL-DA.
 - Transfer contents to a 500 ml separatory funnel.
 - To the funnel, add 13.5 ml of 2 M potassium carbonate (K_2CO_3).
 - Cap the funnel. Gently mix the two layers by inverting the funnel and swirling gently once or twice, taking care to release pressure via the stopcock. Repeat 3 times.
 - Replace the cap with a layer of Parafilm and allow the mixture to separate O/N (~12 hr).
 - Collect the bottom, organic layer into a 250 ml Erlenmeyer flask.
 - Add ~5 g of anhydrous magnesium sulfate ($MgSO_4$) to the flask and gently swirl.
 - Gravity filter the mixture through qualitative filter paper and into a clean 250 ml round bottom flask.
 - Using a rotary evaporator, remove DCM solvent from the flask.
 - Dry under high vacuum to remove residual DCM. (Note: PCL-DA should be stored away from light.)
 - Confirm acrylation with 1H NMR^{22,23}.

2. Preparing the SMP Scaffold (Figure 1)

- Prepare the fused salt template.
 - Use a 425 μm sieve to obtain sodium chloride (NaCl) particles $\sim 460 \pm 70$ μm in diameter. (Note: Average particle size may be confirmed from scanning electron microscopy [SEM] images with ImageJ software.)¹⁴

2. To a 3 ml glass vial (I.D. = 12.9 mm), add 1.8 g of the previously sieved NaCl.
3. Slowly add, in four portions, 7.5 wt% (based on salt weight) DI water (0.146 g) to the vial. Mix with a metal spatula after the addition of each portion of water.
4. Cap the vial, wrap in tissue and place vertically into a centrifuge tube. Centrifuge for 15 min at 3,220 x g.
5. Remove the cap and let air-dry O/N (~12 hr).
2. In a new glass vial, prepare a "macromer solution" by combining 0.15 g of PCL-DA per ml of DCM. (Note: For one scaffold, ~ 1 ml of solution should be prepared.) Cap and mix the solution at high speed on a vortex mixer for ~1 min.
3. In a new 3 ml glass vial, prepare a "photoinitiator solution" based on 10 wt% 2,2-dimethoxy-2-phenyl acetophenone (DMP) in 1-vinyl-2-pyrrolidinone (NVP). Combine 0.115 g of DMP in 1 ml of NVP. (Note: For one scaffold, ~180 μ l is required.) Cap, wrap in aluminum foil (to block light) and mix the solution at high speed on a vortex mixer for ~1 min. (Note: If prepared in advanced, the solution should be refrigerated and protected from light.)
4. Wrap the vial containing the macromer solution (excluding the cap) with aluminum foil (to block light) and add via pipette 15 vol% (based on total volume of the macromer solution) of the photoinitiator solution. Cap and mix the solution at high speed on a vortex mixer for ~1 min.
5. Wrap the vial containing the fused salt template (excluding the cap) with aluminum foil (to block light) and add via pipette the previously prepared macromer/photoinitiator solution (~0.6 ml or until the template is completely covered).
6. Cap the vial, wrap in tissue and place vertically into a centrifuge tube. Centrifuge for 10 min at 1,260 x g to distribute the macromer solution throughout the template.
7. Remove the aluminum foil, uncap the vial and expose to UV light (365 nm, 25 W) for 3 min. Air-dry O/N.
8. Remove the "salt-containing scaffold" from the vial with tweezers after scoring and fracturing the top of the glass vial.
9. In a 400 ml beaker, prepare ~200 ml of a water/ethanol solvent (1:1 vol:vol).
10. Maintain the scaffold submerged in the water/ethanol solvent for 4 days with daily solvent changes.
11. Remove the scaffold from the solvent and air-dry O/N.

3. Applying Polydopamine Coating to SMP Scaffold (Figure 1)

1. In 400 ml beaker equipped with a Teflon-covered stir bar, prepare ~200 ml of a dopamine hydrochloride solution (2 mg/ml in 10 mM Tris buffer, pH = 8.5, 25 °C). Stir at ~150 rpm.
2. Place a disposable needle (length = 40 mm; gauge = 20) into the scaffold, ~half the distance through the scaffold. Wrap a wire around the needle hub.
3. Submerge the scaffold (with the needle hub above the solution surface) into the stirring dopamine solution by anchoring the wire to the rim of the beaker.
4. Degas the scaffold by placing a syringe into the needle hub and using it to pull air out of the scaffold. (Note: Degassing is complete when no more air can be removed and the solution has completely infiltrated the scaffold.)
5. Maintain the scaffold submerged in the stirring dopamine solution for 16 hr.
6. Remove the scaffold from the solution and remove the needle. Rinse with DI water and dry in a vacuum oven at RT for 24 hr.
7. Place the scaffold in an 85 °C oven for 1 hr.
8. Allow the scaffold to cool to RT. The final cylindrical scaffold will be ~6 mm diameter x ~5 mm height.

4. Evaluating "Self-fitting" Behavior

1. Prepare an "irregular CMF defect model" using a sheet of rigid plastic whose thickness is ~5 mm. Use a drill to create a void within the plastic sheet with an average diameter slightly less than ~6 mm, as demonstrated in **Figure 2A**.
2. In a beaker, heat DI water (representing the clinical use of saline) to a temperature of ~60 °C.
3. Place the scaffold into the beaker of ~60 °C water. Use tweezers to push the scaffold below the water surface, exposing all areas to the water. Continue for ~2 min or until the scaffold is noticeably softened (**Figure 2B**).
4. Remove the scaffold from the beaker and immediately press (by hand) into the model defect.
5. Allow to cool to RT (~5-10 min) (**Figure 2C**).
6. Remove from the defect to observe the new, fixed temporary shape and the return of the relatively more rigid state (**Figure 2D**).

5. Testing Shape Memory Behavior

1. Using a dynamic mechanical analyzer (DMA; e.g. a TA Instruments Q800 as used herein), run a strain-controlled cyclic-thermal mechanical compression test on a scaffold over two cycles (N) to determine shape fixity (R_f) and shape recovery (R_r) (**Figure 3**).
 1. Equilibrate to 60 °C (T_{high}) for 5 min.
 2. Compress to a maximum strain (ϵ_m = 50 %) at 50 %/min.
 3. Hold at ϵ_m (5 min).
 4. Cool to 25 °C (T_{low}) and maintain for 10 min to fix the temporary shape.
 5. Remove the load.
 6. Measure the ultimate strain in the stress-free state (ϵ_u).
 7. Reheat to 60 °C (T_{high}) and maintain for 10 min to recover the permanent shape.
 8. Measure the recovered strain (ϵ_p).
 9. While still at 60 °C (T_{high}), start the 2nd cycle (N = 2) by compressing the scaffold to 50 % of the height recovered after the 1st cycle (N = 1).
 10. Repeat 5.1.3-5.1.8 for N = 2.
 11. Calculate R_f and R_r for N = 1 and 2 using the following equations:

$$R_f(N) = [\varepsilon_u(N) / \varepsilon_m] R_r(N) = [\varepsilon_m - \varepsilon_p(N)] / [\varepsilon_m - \varepsilon_p(N-1)]$$

6. Visualizing Pore Size and Pore Interconnectivity

- Using scanning electron microscopy (SEM; e.g. a FEI Quanta SEM as used herein), observe the pore size and pore interconnectivity.
 - Using tweezers to hold the SMP scaffold, submerge in liquid N₂ for 1 min.
 - Remove from liquid N₂ and fracture along the middle of the scaffold with a clean razor blade.
 - Using carbon tape, affix one of the SMP scaffold halves onto the sample stage with the fractured surface facing up.
 - Sputter coat with Au-Pt (~4 nm).
 - Capture the SEM image at a recommended accelerating voltage of 10-15 kV (**Figure 4A**).

7. Testing of *in vitro* Bioactivity

- Into a 50 ml centrifuge tube, add ~30 ml of 1X SBF²⁴.
- Obtain a scaffold in its original, cylindrically-molded permanent shape. Cut the scaffold in half (across the circular edge) using a clean blade.
- Place an individual scaffold half into the prepared centrifuge tube and cap.
- Maintain the tube at 37 °C in a water bath under static conditions with no SBF changes.
- After 14 days, remove the scaffold from the SBF and air dry for 24 hr.
- Using carbon tape, affix the scaffold onto the sample stage with the fractured surface facing up.
- Sputter coat with Au-Pt (~4 nm).
- Capture the SEM image at a recommended accelerating voltage of 10-15 kV (**Figure 4B**).

Representative Results

The resulting PCL-based SMP scaffold is capable of self-fitting into a model CMF defect (**Figure 2**). After brief exposure to warm saline (~60 °C), the cylindrical scaffold softens allowing the scaffold to be manually pressed into and expand within the model defect. After cooling to RT, the scaffold is fixed into its new temporary shape which is retained upon removal from the defect.

The shape memory behavior of an SMP scaffold is quantified by strain-controlled cyclic-thermal mechanical compression tests in terms of shape fixity (R_f) and shape recovery (R_r) (**Figure 3**). For this PCL-based SMP scaffold, values (%) for cycles N=1 and 2 are: $R_f(1) = 102.5 \pm 0.7$, $R_f(2) = 101.8 \pm 0.3$, $R_r(1) = 95.3 \pm 0.9$, and $R_r(2) = 99.8 \pm 0.2$ ⁶.

The SMP scaffold displays a highly interconnected pore morphology as observed by SEM imaging (**Figure 4A**). This was achieved by the use of a fused salt template, formed by the addition of a small amount of water to the sieved salt (**Figure 1**).

Following exposure to simulated body fluid (SBF; 1X) for 14 days, SEM imaging confirms the formation of HAp (**Figure 4B**) thereby indicating scaffold bioactivity.

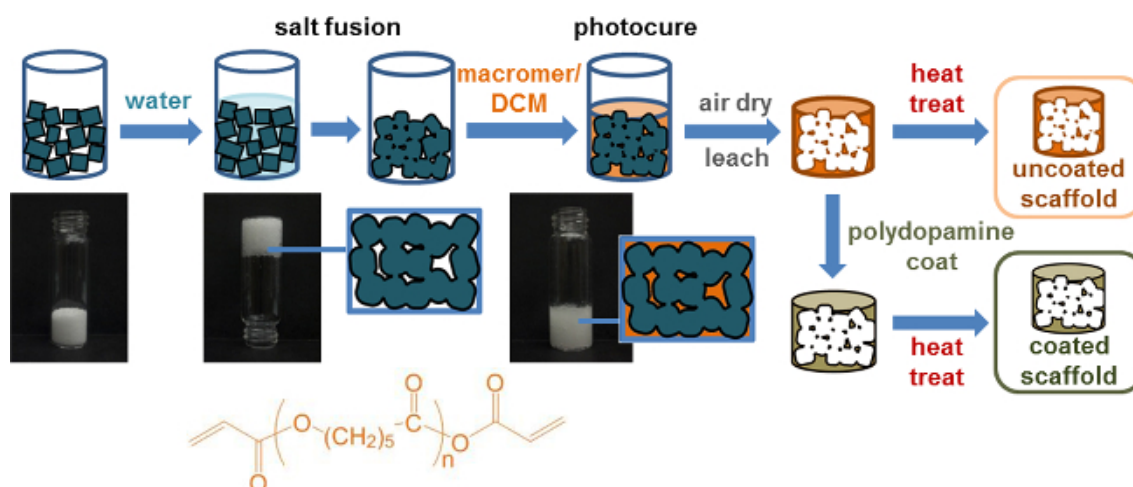


Figure 1. Schematic for preparation of SMP scaffold coated with polydopamine. ASMP scaffold is fabricated via the described protocol based on the photochemical cure of polycaprolactone diacrylate (PCL-DA) using a solvent-casting particulate-leaching (SCPL) method employing fused salt template and application of a bioactive polydopamine coating. The final heat treatment at 85 °C ($T > T_{trans}$) induces scaffold densification. [Please click here to view a larger version of this figure.](#)

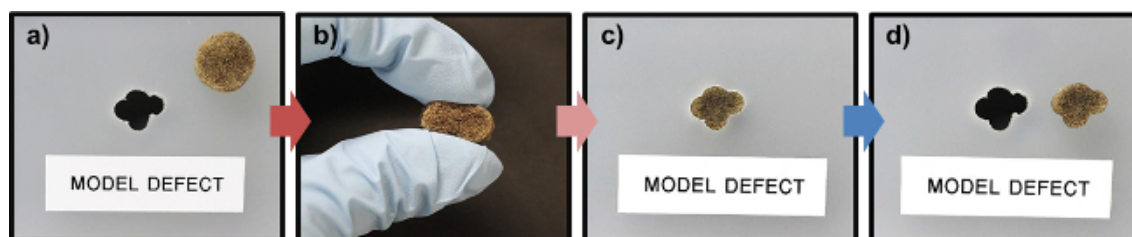


Figure 2. Observation of self-fitting behavior. A cylindrical SMP scaffold (~6 mm diameter x ~5 mm height) is fitted within an “irregular defect model” (A) as follows. Upon heating in water at ~60 °C ($T > T_{trans}$), the scaffold softens and becomes malleable (B) and thus can be mechanically pressed (“fitted”) within the model defect (C). Following cooling to RT, the SMP scaffold is removed and retains its new, fixed temporary shape (D). Upon subsequent heating at ~60 °C, the scaffold undergoes shape recovery to the original, generic cylindrical shape. [Please click here to view a larger version of this figure.](#)

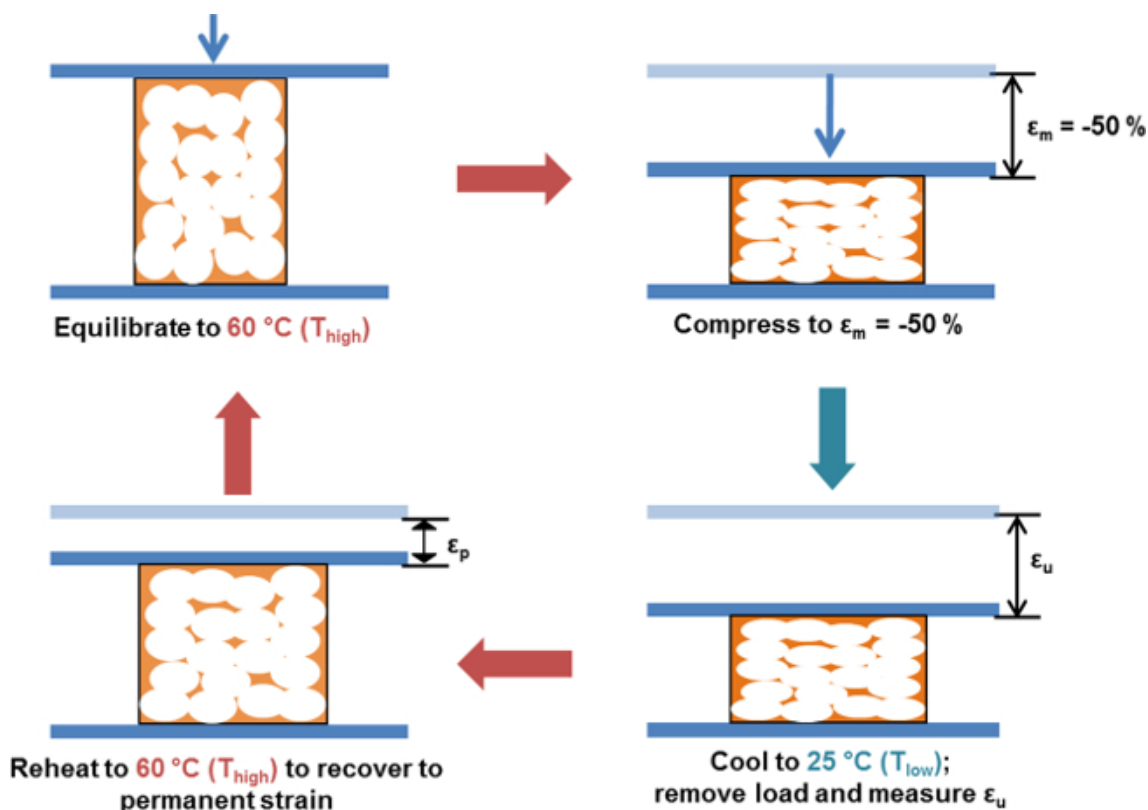


Figure 3. Measurement of shape memory behavior. The shape memory behavior of a SMP scaffold is quantified through a strain-controlled cyclic-thermal mechanical compression test on a scaffold to determine shape fixity (R_f) and shape recovery (R_r) based on measurements of ϵ_m , ϵ_u , and ϵ_p . [Please click here to view a larger version of this figure.](#)

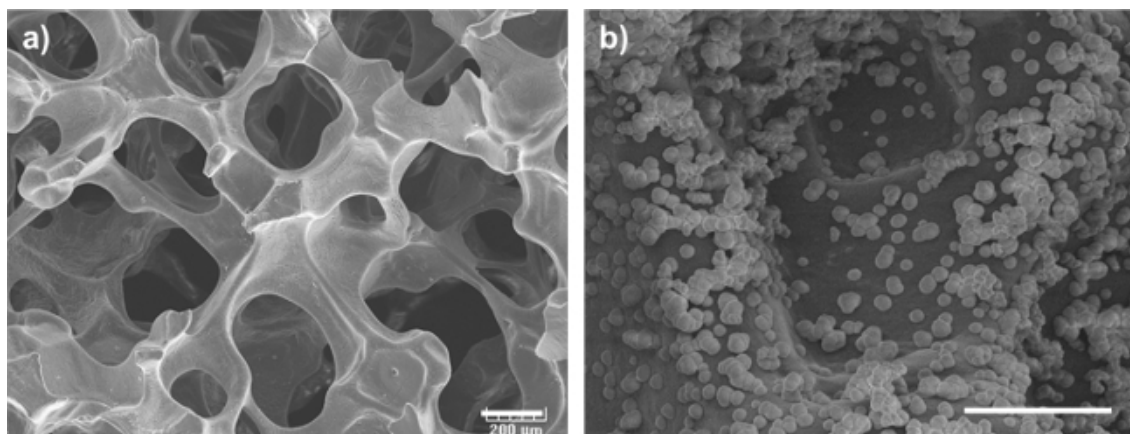


Figure 4. Observation of pore interconnectivity and formation of hydroxyapatite (HAp). Representative SEM images of an uncoated, heat treated SMP scaffold (scale bar = 200 μm) (A) and coated, heat treated scaffold after exposure to SBF (1X) for 14 days (scale bar = 50 μm) (B). Please click here to view a larger version of this figure.

Discussion

This protocol describes the preparation of a polydopamine-coated, PCL-based scaffold whose self-fitting behavior, as well as osteoinductivity and bioactivity, makes it of interest in the treatment of irregular CMF bone defects. Aspects of the protocol may be altered to change various scaffold features.

The protocol begins with acrylation of a PCL-diol to permit UV cure. In the reported example, the PCL-diol M_n is $\sim 10,000$ g/mol. However, by appropriately adjusting amount of acryloyl chloride and Et_3N used during the synthesis of PCL-DA, a PCL diol with a higher or lower M_n may be utilized to decrease or increase, respectively, the crosslink density.

The fused salt template is an important component to the protocol (**Figure 1**). The average salt size determines the resulting scaffold pore size. In the described example, the average salt size was $\sim 460 \pm 70$ μm . While a smaller salt size may be utilized, it should be kept in mind that the scaffold undergoes shrinkage during the final heat treatment step which will reduce pore size. Sieving of the salt is utilized to decrease the salt size distribution and, therefore, the pore size distribution. To produce a scaffold with highly interconnected pores, salt fusion was induced by the addition of a small amount of water (7.5 wt% based on salt weight). This is known to partially dissolve isolated NaCl particles into a continuous poragen template^{25,26}. Depending on the average salt size, the amount water added must be adjusted¹⁴. Furthermore, during salt fusion, the water must be added gradually, mechanical mixed and finally centrifuged to ensure its even distribution as well as the packing of the salt particles.

Having formed the fused salt template, the PCL-DA is dissolved in DCM for solvent-casting. In the described protocol, a concentration of 0.15 g of PCL-DA per 1 ml of DCM was utilized. This concentration may be increased or decreased. However, while increasing concentrations is expected to increase scaffold modulus, it can also produce scaffolds with lower pore interconnectivity¹⁴.

Once the precursor solution has been added onto the salt mold, centrifugation is helpful to aide in its diffusion into the template. Following rapid UV cure, air drying permits evaporation of the DCM solvent. After removal from the mold, the scaffold is soaked in water/ethanol (1:1 vol:vol) for 4 days to remove the salt template. SEM imaging confirms the formation of a highly interconnected pore morphology (**Figure 4A**).

A polydopamine coating is applied to the pore walls of the scaffold to impart bioactivity. Due to the resulting scaffold shrinkage, it is best to apply the coating before the final heat treatment step⁶. In addition, degassing the scaffold while submerged in the aqueous dopamine solution assists infiltration. The degassed scaffold remains submerged in the solution to facilitate uniform polydopamine coverage. Once coated and thoroughly rinsed, the previously white scaffold exhibits a brown color characteristic of polydopamine²¹. Thus, coverage throughout the scaffold can be assessed by visual inspection by halving a scaffold to confirm polydopamine diffusion.

After application of the polydopamine coating, a final heat treatment is performed (85 $^{\circ}\text{C}$, 1 hr). As noted, this process results in scaffold shrinkage. However, heat treatment is essential to achieving shape memory behavior¹⁴, perhaps due to reorganization of the PCL crystalline domains (i.e. switching segments) in closer proximity.

As shown in **Figure 2**, the SMP scaffold achieved self-fitting in a model defect due to its thermoresponsive shape memory nature. Exposure to warm saline (~ 60 $^{\circ}\text{C}$) induced melting of the PCL crystalline domains, such that the softened scaffold could be pressed into the model defect. When the manual pressure was released, the shape recovery promoted expansion of the scaffold to fill the irregular boundaries. Upon cooling to RT, the PCL crystalline domains reformed, fixing the scaffold into its new temporary shape which was retained upon removal from the defect. Previously, we confirmed that the pores along the edges of the removed scaffold remained quite open despite contact with the mold⁶.

When measured by strain-controlled cyclic-thermal mechanical compression tests (**Figure 3**), ideal shape memory behavior is characterized by R_f and R_r values of 100 %. For the described SMP scaffold, R_f values for cycles 1 and 2 were slightly > 100 %⁶. R_f has been previously observed to be slightly greater than 100 %^{14,27} due to a slight increase in compressive strain during shape fixation from the recrystallization of PCL segments into more compact structures²⁷ or from compression-induced recrystallization of PCL. In addition, R_r increased from cycle 1

to cycle ²⁶. An increase in R_f values has been previously noted for solid^{28,29,22} and porous SMPs^{13,14,23}. It is thought that during the first cycle, residual strain originating from processing is removed such that shape recovery increases in the next cycle⁷.

The described tissue engineering scaffold achieves the specific set of properties critical for the successful treatment of CMF bone defects. The scaffold is expected to facilitate osseointegration through its ability to “self-fit” within an irregular CMF bone defect. Osteoconductivity is predicted based on the achieved pore interconnectivity as well as scaffold biodegradability. Finally, due to the polydopamine coating, the scaffold is bioactive as indicated by the formation of HA during *in vitro* tests (**Figure 4B**). This bioactivity is predicted to facilitate integration and bonding with surrounding bone tissue. Thus, this scaffold represents an alternative to autografting and conventional bone substitutes for CMF bone defect repair.

Disclosures

The authors have nothing to disclose.

Acknowledgements

The authors thank Texas A&M University Engineering and Experiment Station (TEES) for financial support of this research. Lindsay Nail gratefully acknowledges support from the Texas A&M University Louis Stokes Alliance for Minority Participation (LSAMP) and the National Science Foundation (NSF) Graduate Research Fellowship Program (GRFP). Dawei Zhang thanks the Texas A&M University Dissertation Fellowship.

References

1. Neovius, E., & Engstrand, T. Craniofacial reconstruction with bone and biomaterials: review over the last 11 years. *J. Plast. Reconstr. Aesthet. Surg.* **63**, 1615-1623, doi: 10.1016/j.bjps.2009.06.003 (2010).
2. Elsalanty, M.E., & Genecov, D.G. Bone grafts in craniofacial surgery. *Cranio-maxillofac. Trauma Reconstr.* **2**, 125-134, doi: 10.1055/s-0029-1215875 (2009).
3. Hollister, S.J., *et al.* Engineering craniofacial scaffolds. *Orthod. Craniofacial Res.* **8**, 162-173, doi: 10.1111/j.1601-6343.2005.00329.x (2005).
4. Albrektsson, T., & Johansson, C. Osteoinduction, osteoconduction and osseointegration. *Eur Spine J.* **10**, S96-S101, doi: 10.1007/s005860100282 (2001).
5. Blokhuis, T. J., & Arts, J. J. C. Bioactive and osteoinductive bone graft substitutes: Definitions, facts and myths. *Injury.* **42**, S26-S29, doi: 10.1016/j.injury.2011.06.010 (2011).
6. Zhang, D., *et al.* A bioactive “self-fitting” shape memory polymer scaffold with potential to treat cranio-maxillo facial bone defects. *Acta Biomater.* **10**, 4597-4605, doi: 10.1016/j.actbio.2014.07.020 (2014).
7. Lendlein, A., & Kelch, S. Shape-memory polymers. *Angew. Chem. Int. Ed.* **41**, 2034-2057, doi: 10.1002/1521-3773(20020617)41:12<2034::aid-anie2034>3.0.co;2-m (2002).
8. Hu, J., Zhu, Y., Huang, H., & Lu, J. Recent advances in shape-memory polymers: Structure, mechanism, functionality, modeling and applications. *Prog. Polym. Sci.* **37**, 1720-1763, doi: 10.1016/j.progpolymsci.2012.06.001 (2012).
9. Middleton, J.C., & Tipton, A.J. Synthetic biodegradable polymers as orthopedic devices. *Biomaterials.* **21**, 2335-2346, doi: 10.1016/S0142-9612(00)00101-0 (2000).
10. Sun, H., Mei, L., Song, C., Cui, X., & Wang, P. The *in vivo* degradation, absorption and excretion of PCL-based implant. *Biomaterials.* **27**, 1735-1740, doi: 10.1016/j.biomaterials.2005.09.019 (2006).
11. Woodruff, M.A., & Hutmacher, D.W. The return of a forgotten polymer—Polycaprolactone in the 21st century. *Prog. Polym. Sci.* **35**, 1217-1256, doi: 10.1016/j.progpolymsci.2010.04.002 (2010).
12. Wang, S., Lu, L., Gruetzmacher, J.A., Currier, B.L., & Yaszemski, M.J. Synthesis and characterizations of biodegradable and crosslinkable poly(ϵ -caprolactone fumarate), poly(ethylene glycol fumarate), and their amphiphilic copolymer. *Biomaterials.* **27**, 832-841, doi: 10.1016/j.biomaterials.2005.07.013 (2006).
13. Zhang, D., Petersen, K.M., & Grunlan, M.A. Inorganic-organic shape memory polymer (SMP) foams with highly tunable properties. *ACS Appl. Mater. Interfaces.* **5**, 186-191, doi: 10.1021/am302426e (2012).
14. Zhang, D., Burkes, W.L., Schoener, C.A., & Grunlan, M.A. Porous inorganic-organic shape memory polymers. *Polymer.* **53**, 2935-2941, doi: 10.1016/j.polymer.2012.04.053 (2012).
15. Van der Stok, J., Van Lieshout, E.M., El-Massoudi, Y., Van Kralingen, G.H., & Patka, P. Bone substitutes in the Netherlands—a systematic literature review. *Acta Biomater.* **7**, 739-750, doi: 10.1016/j.actbio.2010.07.035 (2011).
16. Lee, H., Dellatore, S.M., Miller, W.M., & Messersmith, P.B. Mussel-inspired surface chemistry for multifunctional coatings. *Science.* **318**, 426-430, doi: 10.1126/science.1147241 (2007).
17. Hong, S., *et al.* Non-covalent self-assembly and covalent polymerization co-contribute to polydopamine formation. *Adv. Funct. Mater.* **22**, 4711-4717, doi: 10.1002/adfm.201201156 (2012).
18. Ryu, J., Ku, S.H., Lee, H., & Park, C.B. Mussel-inspired polydopamine coating as a universal route to hydroxyapatite crystallization. *Adv. Funct. Mater.* **20**, 2132-2139, doi: 10.1002/adfm.200902347 (2010).
19. Lee, Y.B., *et al.* Polydopamine-mediated immobilization of multiple bioactive molecules for the development of functional vascular graft materials. *Biomaterials.* **33**, 8343-8352, doi: 10.1016/j.biomaterials.2012.08.011 (2012).
20. Wu, C., Fan, W., Chang, J., & Xiao, Y. Mussel-inspired porous SiO₂ scaffolds with improved mineralization and cytocompatibility for drug delivery and bone tissue engineering. *J. Mater. Chem.* **21**, 18300-18307, doi: 10.1039/C1JM12770E (2011).
21. Ku, S.H., Ryu, J., Hong, S.K., Lee, H., & Park, C.B. General functionalization route for cell adhesion on non-wetting surfaces. *Biomaterials.* **31**, 2535-2541, doi: 10.1016/j.biomaterials.2009.12.020 (2010).
22. Schoener, C.A., Weyand, C.B., Murthy, R., & Grunlan, M.A. Shape memory polymers with silicon-containing segments. *J. Mater. Chem.* **20**, 1787-1793, doi: 10.1039/B924032B (2010).

23. Zhang, D., Giese, M.L., Prukop, S.L., & Grunlan, M.A. Poly(ϵ -caprolactone)-based shape memory polymers with variable polydimethylsiloxane soft segment lengths. *J. Polym. Sci. Pol. Chem.* **49**, 754-761, doi: 10.1002/pola.24488 (2011).
24. Kokubo, T., Takadama, H. How useful is SBF in predicting *in vivo* bone bioactivity? *Biomaterials*. **27**, 2907-2915, doi: 10.1016/j.biomaterials.2006.01.017 (2006).
25. Murphy, W.L., Dennis, R.G., Kileny, J.L., & Mooney, D.J. Salt fusion: an approach to improve pore interconnectivity within tissue engineering scaffolds. *Tissue Eng.* **8**, 43-52, doi: 10.1089/107632702753503045 (2002).
26. Yang, Q., Chen, L., Shen, X., & Tan, Z. Preparation of polycaprolactone tissue engineering scaffolds by improved solvent casting/particulate leaching method. *J. Macromol. Sci. Phys.* **45**, 1171-1181, doi: 10.1080/00222340600976783 (2006).
27. Madbouly, S.A., Kratz, K., Klein, F., & Lüzow, K., Lendlein, A. Thermomechanical behaviour of biodegradable shape-memory polymer foams. **1190** 2009 MRS Spring Meeting. Mater. Res. Soc. Symp. Proc. (2009).
28. Luo, X., & Mather, P.T. Preparation and characterization of shape memory elastomeric composites. *Macromolecules*. **42**, 7251-7253, doi: 10.1021/ma9015888 (2009).
29. Lendlein, A., Schmidt, A.M., & Langer, R. AB-polymer networks based on oligo(ϵ -caprolactone) segments showing shape-memory properties. *Proc. Natl. Acad. Sci.* **98**, 842-847, doi: 10.1073/pnas.98.3.842 (2001).